Journal of Mammary Gland Biology and Neoplasia (2019) 24:305–321
https://doi.org/10.1007/s10911-019-09437-z

Exogenous ERα Expression in the Mammary Epithelium Decreases Over Time and Does Not Contribute to p53-Deficient Mammary Tumor Formation in Mice

Lisette M. Cornelissen[1] · Linda Henneman[1,2] · Anne Paulien Drenth[1] · Eva Schut[1] · Roebi de Bruijn[1,3] · Sjoerd Klarenbeek[4] · Wilbert Zwart[5,6] · Jos Jonkers[1]

Received: 18 June 2019 / Accepted: 9 October 2019 / Published online: 15 November 2019

Abstract

Approximately 75% of all breast cancers express the nuclear hormone receptor estrogen receptor α (ERα). However, the majority of mammary tumors from genetically engineered mouse models (GEMMs) are ERα-negative. To model ERα-positive breast cancer in mice, we exogenously introduced expression of mouse and human ERα in an existing GEMM of p53-deficient breast cancer. After initial ERα expression during mammary gland development, expression was reduced or lost in adult glands and p53-deficient mammary tumors. Chromatin immunoprecipitation (ChIP)-sequencing analysis of primary mouse mammary epithelial cells (MMECs) derived from these models, in which expression of the ERα constructs was induced in vitro, confirmed interaction of ERα with the DNA. In human breast and endometrial cancer, and also in healthy breast tissue, DNA binding of ERα is facilitated by the pioneer factor FOXA1. Surprisingly, the ERα binding sites identified in primary MMECs, but also in mouse mammary gland and uterus, showed an high enrichment of ERE motifs, but were devoid of Forkhead motifs. Furthermore, exogenous introduction of FOXA1 and GATA3 in ERα-expressing MMECs was not sufficient to promote ERα-responsiveness of these cells. Together, this suggests that species-specific differences in pioneer factor usage between mouse and human are dictated by the DNA sequence, resulting in ERα-dependencies in mice that are not FOXA1 driven. These species-specific differences in ERα-biology may limit the utility of mice for in vivo modeling of ERα-positive breast cancer.

Keywords ERα · Breast cancer · Mouse model · Pioneer factor · ERα-cistrome · Species-specificity

Introduction

Breast cancer is the most common cancer diagnosed and a leading cause of cancer death in women worldwide [1]. About 75% of all breast cancers express estrogen receptor α (ERα), member of the nuclear hormone receptor family [2, 3]. Stimulation of ERα with estrogens drives proliferation in ERα-positive breast cancer cells, but is also important in the development and function of various healthy tissues [4–6]. Estrogens interact with the hormone binding pocket within the ligand-binding domain (LBD) of ERα, resulting in dimerization and subsequent association of the receptor to consensus estrogen response elements (ERE) mediated by the DNA-binding domain (DBD) [5, 7]. Pioneer factors FOXA1 and GATA3 are known to be required for genome-wide DNA interactions of ERα [8–10]. These pioneer factors facilitate DNA interactions of ERα by binding and modulating compacted chromatin, allowing ERα to interact with the DNA. In addition to direct binding to ERE elements, ERα is able to interact indirectly with the DNA by tethering through other transcription factors, such as AP1 and SP1 [11, 12]. Upon DNA binding, two transcription activation functions (AF1 and AF2) regulate transcriptional activity by co-factor recruitment, such as members of the p160/steroid receptor co-activator (SRC) family (SRC1, SRC2 and SRC3) [13–15]. SRC1, SRC2 and SRC3 are capable of recruiting additional

Lisette M. Cornelissen and Linda Henneman contributed equally to this work.

Electronic supplementary material The online version of this article (https://doi.org/10.1007/s10911-019-09437-z) contains supplementary material, which is available to authorized users.

✉ Wilbert Zwart
w.zwart@nki.nl

✉ Jos Jonkers
j.jonkers@nki.nl

Extended author information available on the last page of the article

transcription factors, resulting in assembly of general transcription machinery and recruitment of RNA polymerase II to induce transcriptional activation [16].

To study the etiology of human ERα-positive breast cancer and to investigate endocrine treatment response and resistance mechanisms, suitable in vivo models are required. Unfortunately, limited options are available, of which cell lines or patient-derived xenografts are the most frequently used model systems [17]. Even though these models reflect the estrogen dependency of ERα-positive breast cancer, most of these xenograft models require exogenous 17β-estradiol supplementation to support growth, do not recapitulate the early phases of tumor initiation and require the use of immunocompromised mice [18–20]. The development of genetically engineered mouse models (GEMMs) of ERα-positive breast cancer has proven to be challenging. The vast majority of GEMMs develop ERα-negative breast cancer, and the few models that do develop ERα-positive mammary tumors are mostly not proven to respond to estrogens or endocrine therapy [17, 21]. Therefore, there is a clear unmet need to generate autochthonous models of ERα-driven breast cancer, in order to reliably investigate endocrine therapy response and resistance in vivo.

In this study, we set out to develop GEMMs of ERα-positive breast cancer that recapitulate the human disease etiology. Since *TP53*-mutations are identified as tumor drivers in about 20–30% of ERα-positive breast cancers [22, 23], we introduced mammary gland-specific exogenous expression of mouse or human ERα in an existing GEMM of p53-deficient breast cancer [24, 25]. Even though exogenous ERα was readily expressed during mammary gland development, the p53-deficient tumors that arose were largely ERα-negative. We compared ERα-cistromes in primary mouse mammary epithelial cells (MMECs) derived from these mouse models to the established ERα-cistrome in human cells and identified a lack of Forkhead motifs in the mouse ERα-cistrome. Exogenous expression of FOXA1 in ERα-expressing MMECs was not sufficient to restore estrogen-dependency, implicating that there are species-specific differences dictated by the genome that alter ERα-biology in murine cells.

Materials and Methods

Mouse Models

ERα sequences were isolated from mouse *Esr1* (9830143G19, RIKEN mouse cDNA library, FANTOM3) and human *ESR1* (MHS6278–211691051, GE Dharmacon/Horizon Discovery, Lafayette, CO, USA) cDNA using specific PCR primers with FseI (m*Esr1*) or BamHI (h*ESR1*) and PmeI overhangs using PWO DNA polymerase (11644947001, Sigma-Aldrich, Zwijndrecht, The Netherlands) (primers listed in supplementary Table S1) and subsequently cloned into a zero TOPO blunt vector (450245, ThermoFisher Scientific, Bleiswijk, The Netherlands). Sequence-verified cDNAs were inserted as FseI-PmeI or BamHI-PmeI fragments into the *Frt-inv*CAG-IRES-*Luc* vector [26]. Flp-mediated integration of the shuttle vectors in *Wap-Cre;Trp53*$^{F/F}$*;Col1a1*$^{frt/+}$ ESC clones (FVB) and subsequent blastocyst injections of the modified ESCs were performed as described previously [26]. The resulting chimeric animals were crossed with *Wap-Cre;Trp53*$^{F/F}$ (FVB) animals to generate the cohorts. The *Wap-Cre*, *Trp53*$^{F/F}$, *Col1a1*$^{invCAG\text{-}mESR1\text{-}IRES\text{-}Luc}$, *Col1a1*$^{invCAG\text{-}hESR1\text{-}IRES\text{-}Luc}$, *Col1a1*$^{invCAG\text{-}HA\text{-}mESR1\text{-}IRES\text{-}Luc}$ and *Col1a1*$^{invCAG\text{-}HA\text{-}hESR1\text{-}IRES\text{-}Luc}$ alleles were confirmed by multiplex PCR using MyTaq HS Red Mix (BIO-25048, Bioline, Waddinxveen, The Netherlands) with an annealing temperature of 60 °C, according to manufacturer's instructions. All used primers are listed in supplementary Table S1. E2 pellets, containing 0.18 mg of 17β-estradiol for 90-day slow-release (NE-121, Innovative Research of America, Sarasota, FL, USA), or placebos (NC-111) were implanted in the lateral region of the neck at 5 weeks of age and replaced every 90 days. Mice were monitored twice weekly for the development of palpable tumors. Mice were sacrificed when (total) mammary tumor burden reached a size of 1500 mm^3 (0.5 x length x $width^2$). All mouse experiments were approved by the Animal Ethics Committee of the Netherlands Cancer Institute and performed in accordance with institutional, national and European guidelines for animal care and use.

In Vitro and In Vivo Bioluminescence Imaging

Bioluminescence imaging was performed as described previously [27]. Signal intensity was measured over the region of interest and quantified as flux (photons/s/square-centimeter/sr). To determine the effect of demethylation in vitro, 2 μM 5-Aza-2'deoxycytidine (A3656, Sigma-Aldrich) was added to the cells 48 h before bioluminescence imaging.

Immunohistochemistry

Mouse tissues were formalin-fixed in 10% neutral buffered formalin, embedded in paraffin and sectioned. Immunohistochemical stainings for mouse and human ERα were processed as described previously [27]. Tris/EDTA buffer-based antigen retrieval was used, followed by anti-ERα (SC-542; supplementary Table S2) and subsequent incubation with HRP-conjugated Envision (Dako/Agilent, Amstelveen, The Netherlands) or anti-ERα (SC-543; supplementary Table S2) and subsequent incubation with biotin-conjugated secondary antibody and HRP-conjugated streptavidin-biotin complex (Dako/Agilent). All slides were

digitally processed using the Aperio ScanScope (Aperio, Vista, CA, USA) and captured using ImageScope software (v12.0.0, Aperio). Quantification of ERα signal was performed on 5 fields of view, containing ductal structures, per gland of 12–15 glands per genotype.

Isolation of Primary MMECs

Primary MMECs were isolated as described previously [28, 29]. In brief, mammary glands were harvested from 8 to 15-week-old mice, minced, and incubated for approximately 30 min at 37 °C in collagenase/trypsin solution: DMEM/F12 Glutamax (31331–093, ThermoFisher Scientific) with 1 mg/ml collagenase A (11088793001, Sigma-Aldrich), 3 mg/ml trypsin (#215250, BD Biosciences, Breda, The Netherlands) and 5 μg/ml insulin (I0516, Sigma-Aldrich). Enzyme activity was neutralized by addition of DMEM/F12-Glutamax, containing 2% fetal bovine serum (FBS; F0926, Sigma-Aldrich), and the suspension was dispersed through a 40 μm cell strainer. Suspensions were centrifuged at 1500 rpm, and resuspended 3 times in DMEM/F12-Glutamax. Cells were plated in DMEM/F12-Glutamax, containing 10% FBS, 50 IU/ml penicillin, 50 μg/ml streptomycin (15070–63, ThermoFisher Scientific), 5 μg/ml insulin, 5 ng/ml EGF (E4127, Sigma-Aldrich) and 5 ng/ml cholera-toxin (Inaba 569B, Gentaur, Kampenhout, Belgium). Isolated MMECs were treated with 1-10 × 10^7 IU/ml AdCre (Gene Transfer Vector Core, University of Iowa, USA) 24 h after isolation. MMECs were harvested 72–96 h after AdCre transduction. AdCre-transduced MMECs were not kept in culture, but isolated separately for each experiment.

Cell Lines and Culturing Conditions

Cells were cultured at 37 °C in a 5% CO_2 incubator. MCF7 cells were cultured in DMEM/F12-Glutamax containing 10% FBS, 50 IU/ml penicillin and 50 μg/ml streptomycin. HC11 cells were cultured in RPMI-1640 (21875–091; ThermoFisher Scientific), 50 IU/ml penicillin, 50 μg/ml streptomycin, 10 μg/ml insulin and 10 ng/ml EGF. For hormonal depletion experiments, cells were transferred to phenol red-free DMEM (11880–036, ThermoFisher) containing 5% charcoal-treated FBS (CTS; SH30068.03, ThermoFisher Scientific) for 72 h. HEK293T cells for virus production were cultured in Iscove's modified Dulbecco's medium (I3390, Sigma-Aldrich) containing 10% FBS, 50 IU/ml penicillin and 50 μg/ml streptomycin. All cell lines were routinely tested for mycoplasma contamination using the MycoAlert Mycoplasma Detection Kit (LT07–318, Lonza, Breda, The Netherlands).

Human *ERα*, *FOXA1*, *GATA3*, *SRC1*, *SRC2* and *SRC3* sequences, containing restriction enzyme-specific overhangs (supplementary Table S1), were isolated from MCF7 or T47D cDNA using Q5 High-Fidelity DNA Polymerase (M0492, New England Biolabs, MA, USA) and subsequently cloned into a zero TOPO blunt vector (450245, ThermoFisher Scientific). Sequence-verified cDNAs were isolated using the specific restriction enzymes and inserted into the lentiviral pCDH-CMV-MCS-EF1-puro or pCDH-CMV-MCS-EF1-copGFP (CD510B-1 or CD511B-1 respectively, System Biosciences, CA, USA) vector. Lentiviral particles were produced by co-transfection of four plasmids in HEK293T cells as described previously [30]. Conditioned media containing the lentiviral particles were collected 48 h after transfection and used for transduction. Stable cell lines were obtained after puromycin (1.8 μg/ml; P7255, Sigma-Aldrich) selection.

Protein Analysis

Protein lysates were prepared using RIPA lysis buffer (10 mM Tris-HCl at pH 7.5, 150 mM NaCl, 5 mM EDTA, 0.1% SDS, 1% Triton X-100, 1% deoxycholate in milli-Q) supplemented with protease inhibitors (11836145001, Sigma-Aldrich). Subcellular fractionation was performed using the Subcellular Protein Fractionation Kit for Cultured Cells (78840, ThermoFisher Scientific). Protein lysates or products of cell fractionation were quantified using the BCA Protein Assay Kit (23225, ThermoFisher Scientific). Equal amounts of protein were separated by 4–12% NuPAGE gradient gel (NP0321, ThermoFisher Scientific) and transferred onto nitrocellulose membrane (162–0112, Bio-Rad, Veenendaal, The Netherlands) in transfer buffer (25 mM Tris, 2 M Glycine, 20% Methanol in demineralized water). Membranes were blocked in 5% non-fat dry milk in TBS-T (pH 7.6, 20 mM Tris, 138 mM NaCl, 0.05% Tween-20 in demineralized water) after which they were probed overnight at 4 °C with primary antibodies listed in supplementary Table S2 and 1 h with HRP-conjugated secondary antibodies (1:2000; Dako/Agilent). Protein was visualized using ECL (32209; ThermoFisher Scientific) on film or using the ChemiDoc MP (Bio-Rad).

Immunofluorescence

Cells were fixed using 3.7% paraformaldehyde. Immunofluorescence stainings for mouse and human ERα were performed as described previously, with adaptations [28]. Cells were permeabilized using 1% Triton X-100 and blocking was performed using 5% BSA, followed by incubation with anti-ERα (SC-542 or SC-543; supplementary Table S2). Cells were subsequently incubated with secondary antibody anti-rabbit-AlexaFluor 488 (1:1000, A-11008, ThermoFisher Scientific), stained with Hoechst (1:1000, ThermoFisher Scientific) and mounted using Vectashield (Vector Laboratories H-1000). Images were acquired using a Leica TCS SP5 Confocal and analyzed using LAS AF software (v2.6.3).

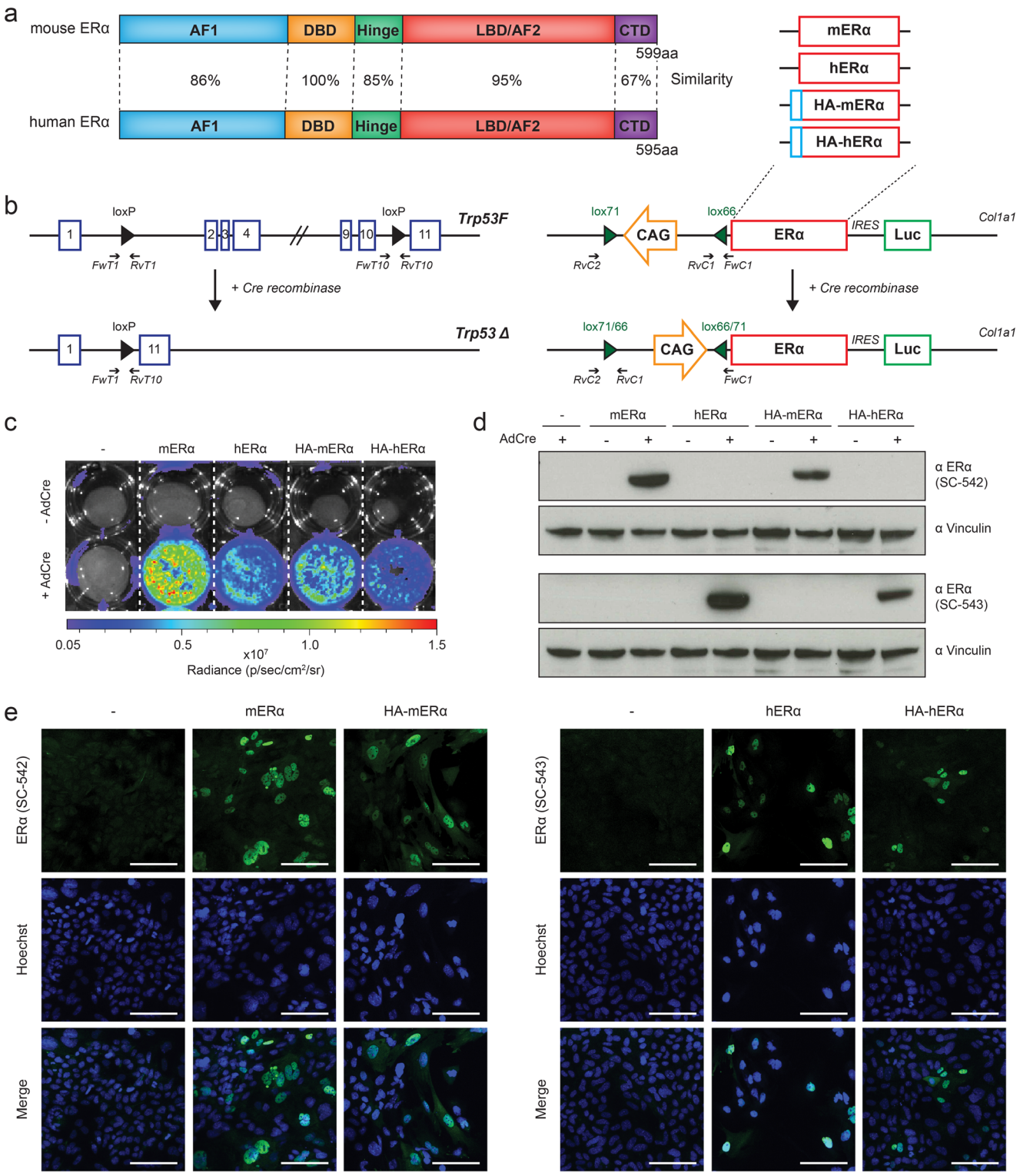

RNA Sequencing

Primary MMECs were hormone deprived for 72 h and treated for 6 h with 10 nM estradiol (E2) or DMSO. Total RNA was extracted from cells using TRIzol reagent (15596026, ThermoFisher Scientific) according to manufacturer's instructions. Quality and quantity of RNA was assessed by the 2100 Bioanalyzer using a Nano chip (Agilent, Santa Clara, CA, USA) and samples having RIN > 8 were subjected to library generation. Library preparation for Illumina sequencing was performed using the Illumina TruSeq RNA Library Preparation kit (RS-122-2001/2, Illumina Inc., San Diego, CA, USA), according

◀ **Fig. 1** Exogenous introduction of mouse or human ERα in *Wap-Cre;Trp53*$^{F/F}$ mice results in nuclear protein expression. **a** Schematic representation of mouse and human ERα. Protein domains and similarity of these domains between mouse and human are indicated. AF1, activation function 1; DBD, DNA binding domain; LBD, ligand binding domain; AF2, activation function 2; CTD, C-terminal domain. **b** Overview of the *Trp53* (*left*) and the *Frt-inv*CAG-*ESR1*-IRES-*Luc* containing *Col1a1* (*right*) locus. Cre recombinase activity results in excision of exons 2–10 of *Trp53* and inversion of the CAG promoter in the *Col1a1* locus, driving expressing of any of the ERα variants in combination with luciferase (Luc). Primers detecting the 5' *loxP* site (FwT1, RvT1), the 3' *loxP* site (FwT10, RvT10) and the deletion of exons 2–10 (FwT1, RvT10) of *Trp53* and the not-recombined (FwC1, RvC1) and recombined (RvC1, RvC2) *Col1a1* locus are indicated. **c** Representative images of bioluminescence imaging of luciferase expression in primary MMECs derived from *Trp53*$^{F/F}$ mice without any construct targeted to the *Col1a1* locus or in combination with mERα, hERα, HA-mERα or HA-hERα, upon recombination induced by adeno-Cre virus (AdCre). **d** Mouse or human ERα expression in primary MMECs derived from the different mouse models (as in **c**) upon AdCre-induced recombination. The HA-tagged proteins run slightly higher than the corresponding untagged proteins. Vinculin was used as loading control. **e** Representative images of mouse (*left*; anti-ERα (mouse), SC-542) and human (*right*; anti-ERα (human), SC-543) ERα expression in AdCre-induced recombined primary MMECs derived from *Trp53*$^{F/F}$, *Trp53*$^{F/F}$*;mERα* and *Trp53*$^{F/F}$*;HA-mERα* mice (*left*) and *Trp53*$^{F/F}$, *Trp53*$^{F/F}$*;hERα* and *Trp53*$^{F/F}$*;HA-hERα* mice (*right*) detected by immunofluorescence. Nuclei were counterstained with Hoechst. Scale bars, 100 μm

to manufacturer's instruction, and pooled equimolar into a 10 nM sequencing stock solution. Libraries were sequenced with 65 base single reads on a HiSeq2500 using V4 chemistry (Illumina Inc.). The reads were mapped to the GRCm38 or GRCh38 reference genomes using TopHat (v2.0.12 [31]; Bowtie v1.0.0 [32]; Samtools 0.1.19 [33]) with settings transcriptome-index and prefilter-multihits after filtering out low complexity and repetitive reads. Gene expression counts were generated by Icount, which is based on HTSeq-count, using gene definitions from Ensembl GRCm38 or GRCh38 [34]. Read counts were corrected for differences in sequencing depth using DESeqs of median-of-ratios and the normalized counts were log2-transformed [35]. A heatmap clustered on estradiol-responsive genes was created using Euclidean distance with complete linkage.

Chromatin Immunoprecipitation (ChIP) Sequencing

ChIP on proliferating cells was performed as described previously [36]. In short, cells were crosslinked in solution A (pH 7.4, 50 mM Hepes, 100 mM NaCl, 1 mM EDTA, 0.5 M EGTA) containing 2 mM DSG for 35 min, formaldehyde was added to a final concentration of 1% and incubated for another 10 min. After addition of glycine (final concentration of 125 mM) to quench the crosslinking reaction and washing with PBS, cells were collected. The Bioruptor Pico (Diagenode SA, Seraing, Belgium) was used for sonication. Antibodies used were anti-HA-tag and anti-ERα (human) (supplementary Table S2) with 100 μl Protein A magnetic beads (10002D, ThermoFisher Scientific).

Immunoprecipitated DNA was processed for library preparation using the KAPA library preparation kit (Part#0801–0303, KAPA Biosystems, Amsterdam, The Netherlands). Sequences were generated by the Illumina HiSeq2500 (using 65 bp reads) and mapped to GRCm37 or GRCh37 reference genomes using Burrows-Wheeler Aligner (BWA, v0.7.5a) with a mapping quality >20. Peak calling was performed using MACS (v1.4 [37]) and DFilter (v1.5 [38]), where only peaks were considered that were shared by both peak callers. Peaks identified in two replicates were used for downstream analysis. Genome browser snapshots were generated using IGV (v2.4.9) and heatmaps using SeqMiner (v1.3.4 [39]). The genomic distributions of binding sites were analyzed using the *cis*-regulatory element annotation system (CEAS) [40]. Enriched motifs were obtained using the SeqPos motif tool in Galaxy Cistrome [41]. Radar plots were generated using the fraction of DNA motifs identified in at least 10% of binding sites.

RNA Isolation and mRNA Expression

Cells were hormone deprived for 72 h and treated with 10 nM E2, 10 nM ICI 182,780 or DMSO for 6 h. Total RNA was extracted from cells using TRIzol reagent according to manufacturer's instructions. RNA was cleaned up using ISOLATE II RNA Mini Kit (BIO-52073, Bioline) and cDNA was synthesized from 1 μg RNA using Tetro cDNA Synthesis Kit (BIO-65043, Bioline) with random hexamer primers. QPCR was performed using SensiMix SYBR low-ROX kit (BIO-QT625, Bioline) on a QuantStudio 6 system (ThermoFisher Scientific). Primer sequences used for mRNA expression analysis are listed in supplementary Table S1.

Clonogenic Assay

Cells were hormone deprived for 72 h and seeded at 10,000 cells per well in 6-wells plates. After 12 h, the medium was refreshed and 10 nM E2, 10 nM ICI 182,780 or DMSO was added. After 7 days, cells were fixed with 4% formalin in PBS and stained with 0.1% crystal violet in demineralized water. Quantification was performed by dissolving the crystal violet in 10% acetic acid in demineralized water and determining the absorbance at 590 nm.

Statistics

Statistical analyses were performed with GraphPad Prism (v7.03). Statistical tests used were one-way ANOVA, two-way ANOVA and Log-rank (Mantel-Cox) test. *P*-values of <0.05 were considered to be significant.

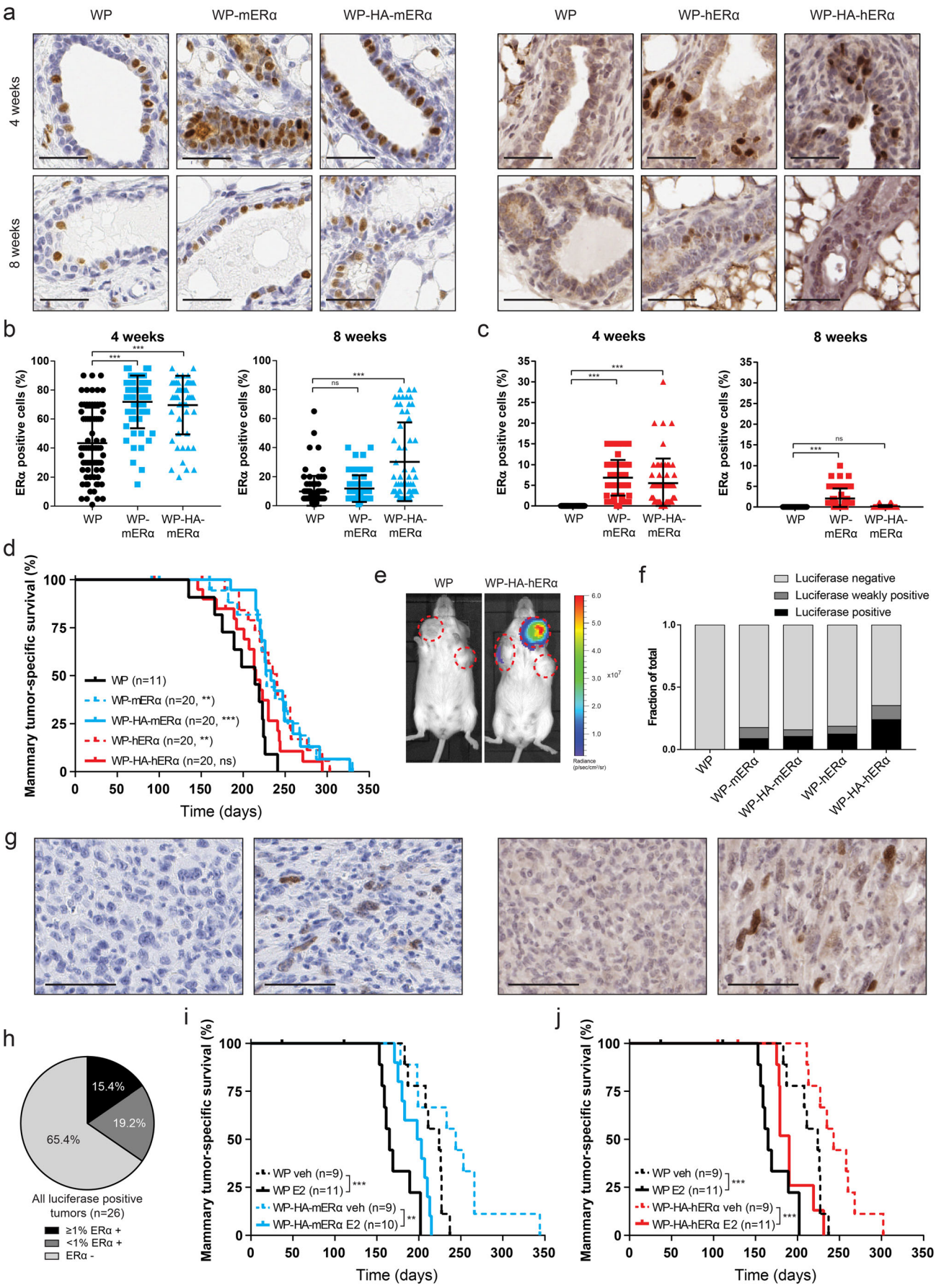
a
WP
WP-mERα
WP-HA-mERα
WP
WP-hERα
WP-HA-hERα
4 weeks
8 weeks
b
4 weeks
8 weeks
ERα positive cells (%)
WP
WP-mERα
WP-HA-mERα
c
4 weeks
8 weeks
ERα positive cells (%)
WP
WP-mERα
WP-HA-mERα
d
Mammary tumor-specific survival (%)
Time (days)
WP (n=11)
WP-mERα (n=20, **)
WP-HA-mERα (n=20, ***)
WP-hERα (n=20, **)
WP-HA-hERα (n=20, ns)
e
WP
WP-HA-hERα
Radiance (p/sec/cm²/sr)
f
Luciferase negative
Luciferase weakly positive
Luciferase positive
Fraction of total
WP
WP-mERα
WP-HA-mERα
WP-hERα
WP-HA-hERα
g
h
15.4%
19.2%
65.4%
All luciferase positive tumors (n=26)
≥1% ERα +
<1% ERα +
ERα -
i
Mammary tumor-specific survival (%)
Time (days)
WP veh (n=9)
WP E2 (n=11)
WP-HA-mERα veh (n=9)
WP-HA-mERα E2 (n=10)
j
Mammary tumor-specific survival (%)
Time (days)
WP veh (n=9)
WP E2 (n=11)
WP-HA-hERα veh (n=9)
WP-HA-hERα E2 (n=11)

◀ **Fig. 2** Overexpression of ERα in a p53-deficiency-driven breast cancer model does not result in mammary tumors with high ERα expression or increased ERα-dependency. **a** Representative microscopic images of mouse ERα (*left*; anti-ERα (mouse), SC-542) and human ERα (*right*; anti-ERα (human), SC-543) expression by immunohistochemistry at 4 and 8 weeks of age. Scale bars, 100 μm. **b**,**c** Percentage ERα-positive cells of WP-mERα and WP-HA-mERα (**b**) or WP-hERα and WP-HA-hERα (**c**) compared to WP at 4 weeks (*left*) and 8 weeks (*right*) of age. Data represent percentage scores of 5 fields of view per gland, containing ductal structures, of 12–15 glands per genotype. ANOVA: *** $p < 0.001$, ns $p > 0.05$. **d** Kaplan-Meier analysis of mammary tumor-specific survival reflecting minor differences between the ERα overexpressing models compared to WP. Mantel-Cox: WP ($n = 11$, 214 days) versus WP-mERα ($n = 20$, 228 days, $p = 0.0053$); WP-HA-mERα ($n = 20$, 233 days, $p = 0.0008$); WP-hERα ($n = 20$, 240 days, $p = 0.0029$); WP-HA-hERα ($n = 20$, 215 days, $p = 0.1610$). *** $p < 0.001$, ** $p < 0.01$, ns $p > 0.05$. **e** Representative images of in vivo bioluminescence imaging of luciferase expression in tumor-bearing mice. Independent tumors are indicated with red dotted circles. **f** Distribution of all palpable tumors separated in luciferase signal being negative, weakly positive and positive. WP-mERα, $n = 34$; WP-HA-mERα, $n = 38$; WP-hERα, $n = 48$; WP-HA-hERα, $n = 54$. **g** Representative microscopic images of tumors that are negative or positive for ERα expression by immunohistochemistry of mouse ERα (*left*; anti-ERα (mouse), SC-542) and human ERα (*right*; anti-ERα (human), SC-543). Scale bars, 100 μm. **h** ERα immunohistochemistry signal classified as ≥1% positive cells, <1% positive cells or negative for all luciferase-positive tumors identified in the different models, shown in **f**. **i**,**j** Kaplan-Meier analysis of mammary tumor-specific survival of WP mice and WP-HA-mERα mice (**i**) or WP-HA-hERα mice (**j**) treated with vehicle (veh) or 17β-estradiol (E2) slow-release pellets. Mantel-Cox: WP E2 ($n = 11$) versus veh ($n = 9$), 165 versus 224 days, $p = 0.0006$; WP-HA-mERα E2 ($n = 10$) versus veh ($n = 9$), 200.5 versus 244 days, $p = 0.0065$; WP-HA-hERα E2 ($n = 11$) versus veh ($n = 9$), 190 versus 243 days, $p = 0.0009$). *** $p < 0.001$, ** $p < 0.01$

Additional experimental details are described in Supplementary materials and methods. All sequencing data generated in this study are available on GEO repository: GSE127863.

Results

Exogenous Introduction of ERα in the Wap-Cre;Trp53$^{F/F}$ Mouse Model Results in Nuclear Protein Expression

Mouse and human ERα show overall an amino acid sequence similarity of 91%, of which the DBD is most conserved domain (100% similarity) and the C-terminal domain (CTD) is least conserved (67%) (Fig. 1a). In our efforts to develop an ERα-positive breast cancer mouse model, we introduced Cre-inducible knock-in alleles of either mouse or human ERα, with or without an HA-tag, in an existing GEMM of p53-deficient breast cancer [24, 25]. To this end, we generated transgenic mice with Cre-inducible expression of any of these ERα variants in combination with firefly luciferase, by targeting *Frt-inv*CAG-*ESR1*-IRES-*Luc* alleles into the *Col1a1* locus of mouse embryonic stem cells (mESCs) derived from *Wap-Cre;Trp53*$^{F/F}$ (WP) mice (Fig. 1b) [26]. Chimeric mice were generated through blastocyst injections of correctly targeted WP mESCs and subsequently crossed back to the WP model, resulting in *Wap-Cre;Trp53*$^{F/F}$*;Col1a1*$^{Frt\text{-}invCAG\text{-}mESR1\text{-}IRES\text{-}Luc}$ (WP-mERα), *Wap-Cre;Trp53*$^{F/F}$*;Col1a1*$^{Frt\text{-}invCAG\text{-}hESR1\text{-}IRES\text{-}Luc}$ (WP-hERα), *Wap-Cre;Trp53*$^{F/F}$*;Col1a1*$^{Frt\text{-}invCAG\text{-}HA\text{-}mESR1\text{-}IRES\text{-}Luc}$ (WP-HA-mERα), *Wap-Cre;Trp53*$^{F/F}$*;Col1a1*$^{Frt\text{-}invCAG\text{-}HA\text{-}hESR1\text{-}IRES\text{-}Luc}$ (WP-HA-hERα) mice, displaying mammary gland-specific loss of p53 combined with overexpression of either mouse or human ERα, with or without an HA-tag.

To confirm whether the human and mouse *ESR1* cDNAs targeted to the *Col1a1* locus encode for functional ERα proteins, primary MMECs were isolated from *Trp53*$^{F/F}$, *Trp53*$^{F/F}$*;mERα*, *Trp53*$^{F/F}$*;hERα*, *Trp53*$^{F/F}$*;HA-mERα* and *Trp53*$^{F/F}$*;HA-hERα* mice. Adeno-Cre virus (AdCre) transduction resulted in efficient recombination of the *Col1a1* and *Trp53* loci (Fig. S1a) and subsequent inversion of the CAG promoter at the *Col1a1* locus driving transcription of any of the *ESR1* cDNAs and luciferase (Fig. 1b), allowing luciferase expression to be used as a proxy for expression of the introduced cDNA. Bioluminescent imaging confirmed luciferase activity in MMECs infected with AdCre (Fig. 1c) and Western blot analyses using antibodies directed at either mouse or human ERα confirmed stable expression of both proteins (Fig. 1d). Nuclear localization of the ERα variants in proliferating MMECs was confirmed by immunofluorescence and subcellular fractionation experiments (Figs. 1e and S1b). Together, these results illustrate efficient Cre-mediated recombination of the conditional *ESR1* knock-in alleles at the *Col1a1* locus, resulting in stable nuclear expression of the introduced ERα variants.

ERα Overexpression Is Lost During Mammary Gland Development and Tumorigenesis

To determine whether the exogenous ERα proteins were overexpressed in mammary glands from WP-mERα, WP-HA-mERα, WP-hERα and WP-HA-hERα mice, females were sacrificed at early age and compared to WP control mice. Immunohistochemistry using the mouse specific ERα antibody showed an higher percentage of ERα-positive luminal cells in the mammary ducts of WP-mERα and WP-HA-mERα mice compared to WP mice at four weeks of age (Fig. 2a,b). Furthermore, human ERα expression was specifically detected in 4-week-old WP-hERα and WP-HA-hERα females, but not in WP mice (Fig. 2a,c). No ERα-positive cells were detected in the mammary ducts of WP mice using the antibody directed at human ERα, indicating that this antibody did not show any cross-reactivity with endogenous mouse ERα (Fig. 2a,c). However, these increased ERα levels were already declining at eight weeks of age (Fig. 2a-c), resulting in a scattered distribution of ERα-

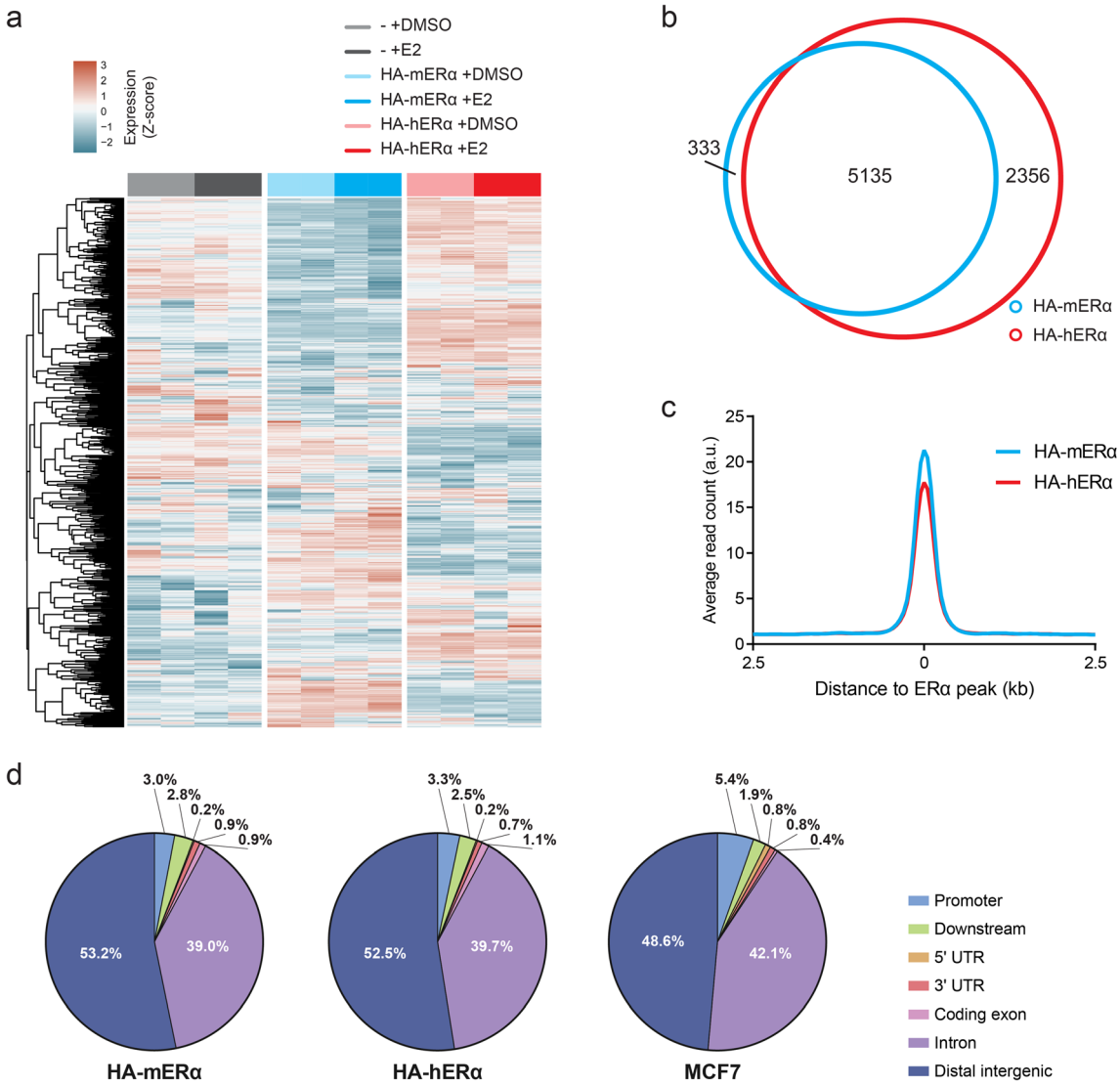

Fig. 3 Exogenous expression of mouse or human ERα in primary MMECs does not sensitize to estradiol stimulation, while both mouse and human ERα interact with the DNA. **a** mRNA expression of primary MMECs derived from *Trp53*$^{F/F}$, *Trp53*$^{F/F}$*;HA-mERα* and *Trp53*$^{F/F}$*;HA-hERα* mice, upon AdCre induced recombination, stimulated with E2 compared to DMSO based on a gene expression signature derived from E2-stimulated MCF7 cells. **b** Venn diagram illustrating the overlap in binding sites identified for HA-mERα and HA-hERα shared in two independent HA-tag directed ChIP-seq experiments in MMECs derived from *Trp53*$^{F/F}$*;HA-mERα* and *Trp53*$^{F/F}$*;HA-hERα* mice, upon AdCre induced recombination. **c** Average read count profiles of the peak signal at all identified HA-mERα and HA-hERα binding sites in AdCre-transduced *Trp53*$^{F/F}$*;HA-mERα* and *Trp53*$^{F/F}$*;HA-hERα* MMECs. **d** Genomic distribution of HA-mERα and HA-hERα binding sites in AdCre-transduced *Trp53*$^{F/F}$*;HA-mERα* and *Trp53*$^{F/F}$*;HA-hERα* MMECs and total ERα binding sites in MCF7 cells

expressing cells, in line with human healthy breast tissue [42, 43]. These results indicate that introducing the different *ESR1* cDNAs in WP mice results in initial overexpression of the corresponding proteins in healthy mammary ducts, but expression of both endogenous and exogenously-introduced ERα is rapidly down-regulated.

Even though ERα overexpression is not maintained in the luminal cells of healthy mammary ducts, ERα-expressing cells might be selected for during outgrowth of p53-deficient tumors. WP, WP-mERα, WP-HA-mERα, WP-hERα and WP-HA-hERα mice were aged to determine whether the presence of any of the ERα constructs affected the latency and/or ERα-status of the developing tumors. WP mice presented multifocal mammary tumors with a median mammary tumor-specific survival of 214 days (Fig. 2d). Exogenous expression of the ERα variants resulted in a modest delay of p53-deficient tumor outgrowth (Figs. 2d and S2a,b). Bioluminescence imaging was performed before tumor-bearing mice were sacrificed to detect whether these tumors showed luciferase activity and therefore were likely to express ERα (Fig. 2e). However, the majority of identified tumors (82.4% in WP-mERα, 84.2% in WP-HA-mERα, 81.3% in

WP-hERα and 64.8% in WP-HA-hERα) were luciferase-negative, indicating that expression of both luciferase and exogenously-introduced ERα was suppressed (Fig. 2f). Of all luciferase-positive tumors ($n = 26$), 19.2% ($n = 5$) showed <1% ERα-positive cells throughout the tumor and 15.4% ($n = 4$) showed ERα expression in ≥1% of tumor cells (Figs. 2g,h and S2b). Cell lines derived from luciferase-negative tumors treated with 5-Aza-2′-deoxycitidine, a DNA demethylating agent, restored luciferase function, suggesting that expression through the CAG promoter was regulated by methylation (Fig. S2c). Together, these results indicate that increased ERα levels did not induce a strong proliferative advantage in p53-deficient mammary epithelial cells, resulting in silencing of ERα expression and outgrowth of ERα-negative cells.

Since estradiol levels in mice are relatively low compared to humans [44], we hypothesized that increasing estradiol levels might promote the proliferative benefit gained by ERα overexpression. Therefore, WP, WP-HA-mERα and WP-HA-hERα animals were treated with 17β-estradiol (E2) or vehicle (veh) slow-release pellets from 5 weeks of age onwards. Tumor onset was stimulated by E2 treatment, as reflected by a decreased mammary tumor-specific survival compared to vehicle treated mice (Fig. 2i,j). However, the decrease in mammary tumor-specific survival was similar for all models (Fig. S2d) and the fraction of luciferase-negative tumors remained high in both E2 and vehicle-treated mice (Fig. S2e; WP-HA-mERα, 77.8% in veh, 80.0% in E2; WP-HA-hERα, 85.7% in veh, 70% in E2). Decreased mammary tumor-specific survival upon E2 stimulation has been described previously in GEMMs of BRCA1-associated triple-negative breast cancer [45]. Collectively, these results suggest that p53-deficient tumor cells in our models do not benefit from ERα expression, independent of E2 stimulation.

DNA Binding Profiles of Mouse or Human ERα in Murine Cells Are Devoid of Forkhead Motifs

To determine whether expression of exogenous ERα affects target gene expression in vitro, RNA-sequencing was performed on AdCre-transduced *Trp53*$^{F/F}$, *Trp53*$^{F/F}$*;HA-mERα* and *Trp53*$^{F/F}$*;HA-hERα* primary MMECs. However, E2 stimulation of ERα-overexpressing MMECs did not affect expression of E2-responsive genes, as identified in hormone-responsive human MCF7 breast cancer cells (Figs. 3a and S3a) [46]. To test whether exogenous ERα in *Trp53*$^{F/F}$*;HA-mERα* and *Trp53*$^{F/F}$*;HA-hERα* primary MMECs was able to interact with DNA, ERα ChIP-sequencing was performed under proliferating conditions using an anti-HA-tag antibody. A similar number of ERα binding sites was identified for both mouse and human ERα ($n = 5468$ and $n = 7491$ respectively) with a comparable signal intensity (Fig. 3b,c). Comparing HA-mERα and HA-hERα binding sites revealed an overlap of 94% (5135 sites; Fig. 3b), but HA-mERα was also detected at HA-hERα specific sites and the other way around, albeit at lower intensities (Fig. S3b,c). Genomic distributions relative to the most-proximal gene of HA-mERα and HA-hERα in MMECs were similar to the genomic distribution of ERα in the human MCF7 cells, with the majority of binding sites detected in intronic and distal intergenic regions (Fig. 3d). This indicates that even though E2 stimulation did not affect known E2-responsive genes, both HA-mERα and HA-hERα do interact with the DNA with a genomic distribution similar to ERα in MCF7 cells.

Even though the overall genomic distribution of ERα, in relation to the most proximal gene, was comparable between HA-mERα and HA-hERα MMECs and MCF7 cells, ERα binding sites at corresponding gene loci were not always similar between mouse and human (Fig. 4a). Some DNA sequences that are conserved between mouse and human were bound by ERα, both in MMECs and MCF7 cells, while other conserved sequences were bound by ERα either in MMECs or MCF7 cells, but not in both. In addition, we observed ERα binding sites in similar regions within a gene in MMECs and MCF7 cells, even though DNA sequences were not conserved. Comparing the DNA motifs identified in genome-wide HA-mERα and HA-hERα binding sites in MMECs and ERα binding sites in MCF7 cells revealed many shared DNA motifs, even though the fraction of binding sites varied, such as the canonical ERE motif (ESR1) recognized by ERα and JUN/FOS motifs indicating tethering through AP-1 (Fig. 4b). However, a subset of DNA motifs identified in MCF7 cells was absent in MMECs, primarily consisting of Forkhead, GATA and Homeobox motifs, specific for factors such as FOXA1 and GATA3; well-known pioneer factors that are considered critical for ERα function in human breast cancer cells [8–10]. We confirmed enrichment of the FOXA1 motif in publicly available ERα ChIP-sequencing datasets of human breast and endometrial tumors [48, 49] and healthy breast tissue [50] (Figs. 4c and S3d). Importantly, publicly available ERα ChIP-seq data of whole mouse mammary gland and E2-stimulated mouse uterus revealed motif enrichments comparable to the enrichments observed in HA-mERα and HA-hERα MMECs, lacking the FOXA1 motif (Figs. 4c and S3d) [51, 52]. In line with the importance of FOXA1 for ERα DNA-binding in human breast cancer [8, 9], a high percentage of ERα binding sites in human tissues and cells contain the FOXA1 motif, while less binding sites contain the canonical ERE motif (Fig. 4c). In contrast, the majority of ERα binding sites in murine tissues and cells contain the ERE motif, but not the FOXA1 motif (Fig. 4c). Furthermore, expression analysis of the factors corresponding to the MCF7-specific motifs revealed high expression of the pioneer factors FOXA1 and GATA3 in MCF7 cells, and relatively low expression in MMECs

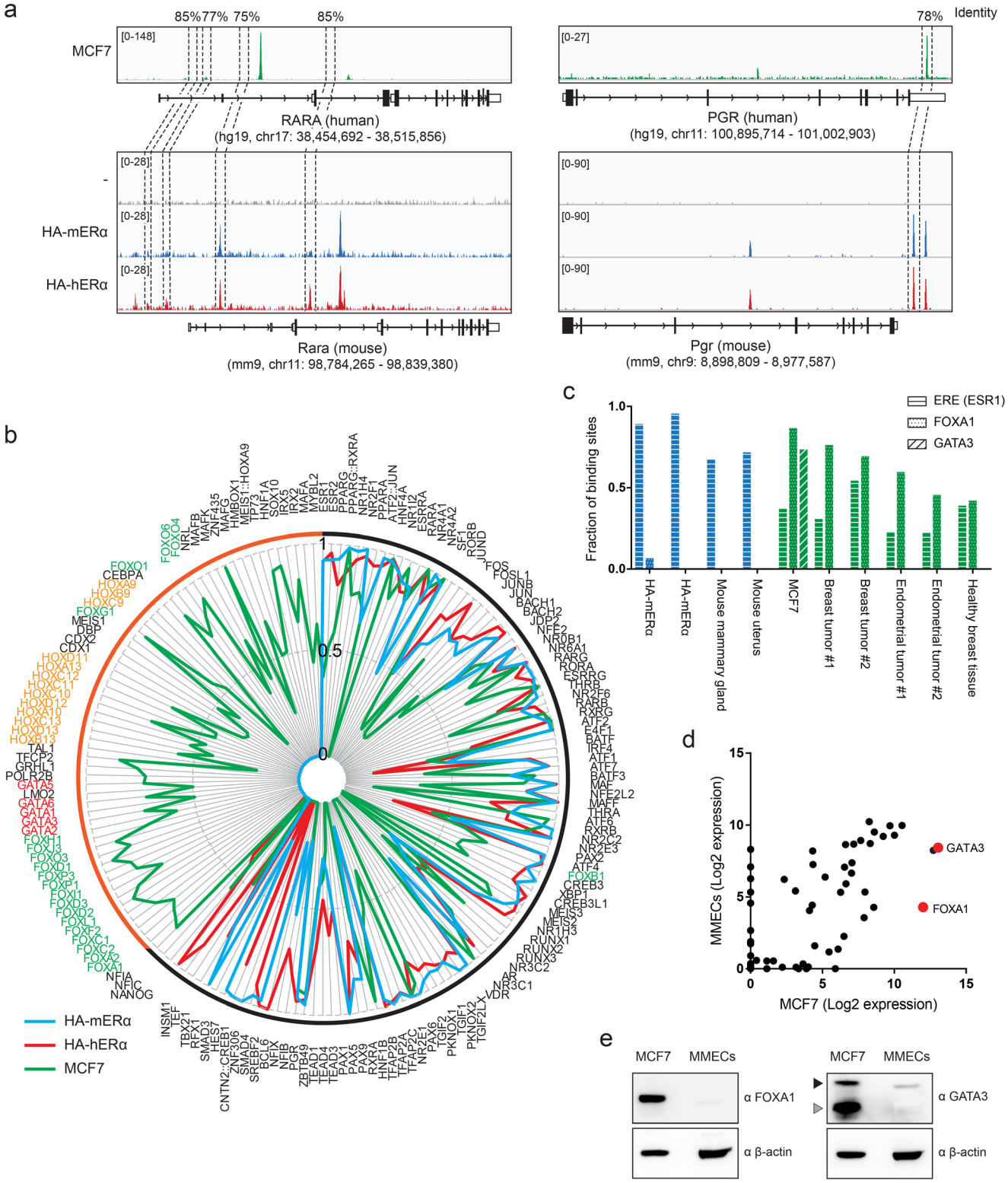

(Figs. 4d,e and S3e). Low expression of these factors might explain the lack of E2-responsiveness upon ERα overexpression, since it has been shown that the human ERα-negative breast cancer cell line MDA-MB-231 can be reprogrammed to restore estrogen-responsive growth by combined exogenous expression of ERα, FOXA1 and GATA3 [53]. Together, these results suggest that insufficient protein levels of FOXA1 and/or GATA3 might explain the non-functional behavior of ERα in WP-ERα and WP-HA-ERα mice and MMECs.

◀ **Fig. 4** DNA binding profiles of both mouse and human ERα in MMECs lack the motif recognized by pioneer factor FOXA1 in contrast to ERα in human cells. **a** Genome browser snapshots of ERα signal in MCF7 cells compared to HA-tag signal in AdCre-transduced *Trp53*$^{F/F}$, *Trp53*$^{F/F}$*;HA-mERα* and *Trp53*$^{F/F}$*;HA-hERα* MMECs. The genomic regions that contain a binding signal and show sequence identity between the mouse and human genomes are indicated with *black* dotted lines. Genomic locations and read counts are indicated. **b** Differential enrichment of the fraction of all DNA motifs identified in at least 10% of binding sites for HA-mERα and HA-hERα in MMECs and total ERα in MCF7 visualized by a radar plot. Motifs specific for ERα in MCF7 are depicted with the orange line. **c** Fraction of ERα binding sites containing the ERE (ESR1), FOXA1 and GATA3 motifs for HA-mERα and HA-hERα in MMECs, mouse mammary gland (GSE43415), E2-stimulated mouse uterus (GSE36455), human MCF7, human breast tumors (GSE40867), human endometrial tumors (GSE94524), and healthy breast tissue (GSE99680). **d** Expression levels of the genes corresponding to the identified MCF-specific motifs shown in **b** for primary MMECs and MCF7 cells. **e** Protein expression levels of FOXA1 and GATA3 in MCF7 cells compared to primary MMECs. β-actin was used as a loading control.Black arrowhead indicates WT GATA3 protein, grey arrowhead indicates truncated GATA3 protein, observed in MCF7 cells [47]

Co-Expression of FOXA1 and GATA3 Does Not Increase ERα-Responsiveness in MMECs

We set out to increase ERα-responsiveness in vitro by transducing the established mouse mammary epithelial cell line HC11 and primary MMECs with cDNAs encoding for ERα, FOXA1 and HA-tagged GATA3, phenocopying the approach used by Kong et al., who described these three factors to be sufficient to induce estrogen-responsive growth in MDA-MB-231 cells [53]. In addition, we introduced human SRC1, SRC2 and SRC3, essential co-activators of ERα [13, 54], of which SRC3 mRNA levels are relatively low in primary MMECs compared to MCF7 cells (Fig. S3f). mRNA expression of the introduced factors could be confirmed in both the HC11 cells and primary MMECs, where the HC11 cells appeared more readily transducible, resulting in consistent expression levels between conditions (Figs. 5a and S4a). Efficient expression of HA-tagged human GATA3 did not increase total human/mouse GATA3 mRNA levels (Fig. 5b), indicating that expression levels are tightly regulated, in line with the established role of GATA3 to act as a tumor suppressor that inhibits growth [55, 56]. Stable protein expression of ERα, FOXA1 and GATA3 was confirmed (Fig. 5c).

We tested ERα-responsiveness of reconstituted HC11 cells and MMECs by determining mRNA expression of two canonical ERα-responsive genes, *Areg* and *Ccnd1* [57, 58], upon treatment with E2 or the ERα degrader fulvestrant (ICI 182,780 [59]) (Figs. 5d and S4b). E2 stimulation minimally affected *Areg* and *Ccnd1* expression in both HC11 cells and MMECs. Only MMECs with highest ERα levels showed a modest inhibition, rather than induction, of both *Areg* and *Ccnd1* expression. ICI treatment resulted in a small decrease of *Ccnd1* expression in HC11 empty vector cells, but a more consistent increase of *Areg* and *Ccnd1* expression in MMECs in multiple conditions. This indicates that in both primary and established MMECs, activation of ERα-signaling can counteract *Areg* and *Ccnd1* expression, while this is alleviated by inhibition of ERα-signaling. In addition, clonogenic growth assays were performed under similar conditions, to determine the impact on cell proliferation capacity (Figs. 5e,f and S4c,d). While no effects were observed with fulvestrant, growth of HC11 cells and MMECs was either unaffected or inhibited upon E2 stimulation in the presence of ERα with or without additional transcription factors. Expression of exogenous FOXA1 decreased clonogenic growth of MMECs and to a lesser extent HC11 cells, in line with previous data showing that FOXA1 expression can be growth inhibitory when it is not in a functional complex with ERα and GATA3 [53]. These data show that combined expression of human ERα, FOXA1, GATA3 and SRC3 is not sufficient to induce ERα-dependency in both primary and established MMECs. Together with the observation that ERα shows FOXA1-independent DNA-binding activity in mouse mammary epithelium and uterus, these results suggest that there are species-specific differences in the DNA sequence that result in differential pioneer factor dependencies.

Discussion

In our efforts to generate novel autochthonous mouse models of ERα-positive breast cancer, we generated mice with mammary gland-specific overexpression of ERα combined with loss of p53, which is common (20–30%) in luminal breast cancer. Even though high ERα levels were observed in developing mammary glands, expression was greatly reduced or absent in adult glands and p53-deficient mammary tumors. DNA interactions of mouse and human ERα in MMECs showed a genomic distribution similar to human ERα in MCF7 cells. However, ERα binding in MMECs was not associated with the transcription factors FOXA1 and GATA3, and exogenous expression of FOXA1 and GATA3 did not induce an ERα-responsive phenotype in ERα-expressing MMECs.

Even though 75% of human breast cancers are ERα-positive, the development of GEMMs of ERα-positive breast cancer remains challenging. To date, several GEMMs have been developed that give rise to ERα-expressing tumors (reviewed in [21]). For example, mammary gland-specific transgenic overexpression of ERα and SV40 large T-antigen induces mammary tumors in 37% of mice, but only a subset displays E2-responsive growth [60]. Overexpression of ERα co-activator AIB1/SRC3 or loss of STAT1 results in ERα-positive mammary tumors in a subset of animals, of which *Stat1*$^{-/-}$ tumor-derived cell lines show E2-responsive growth upon transplantation [61–63]. In addition, mammary gland-specific overexpression of prolactin induces mammary tumors, of which 50% expresses ERα, that are insensitive to estrogen deprivation [64, 65]. About 30% of *Tip30*$^{-/-}$

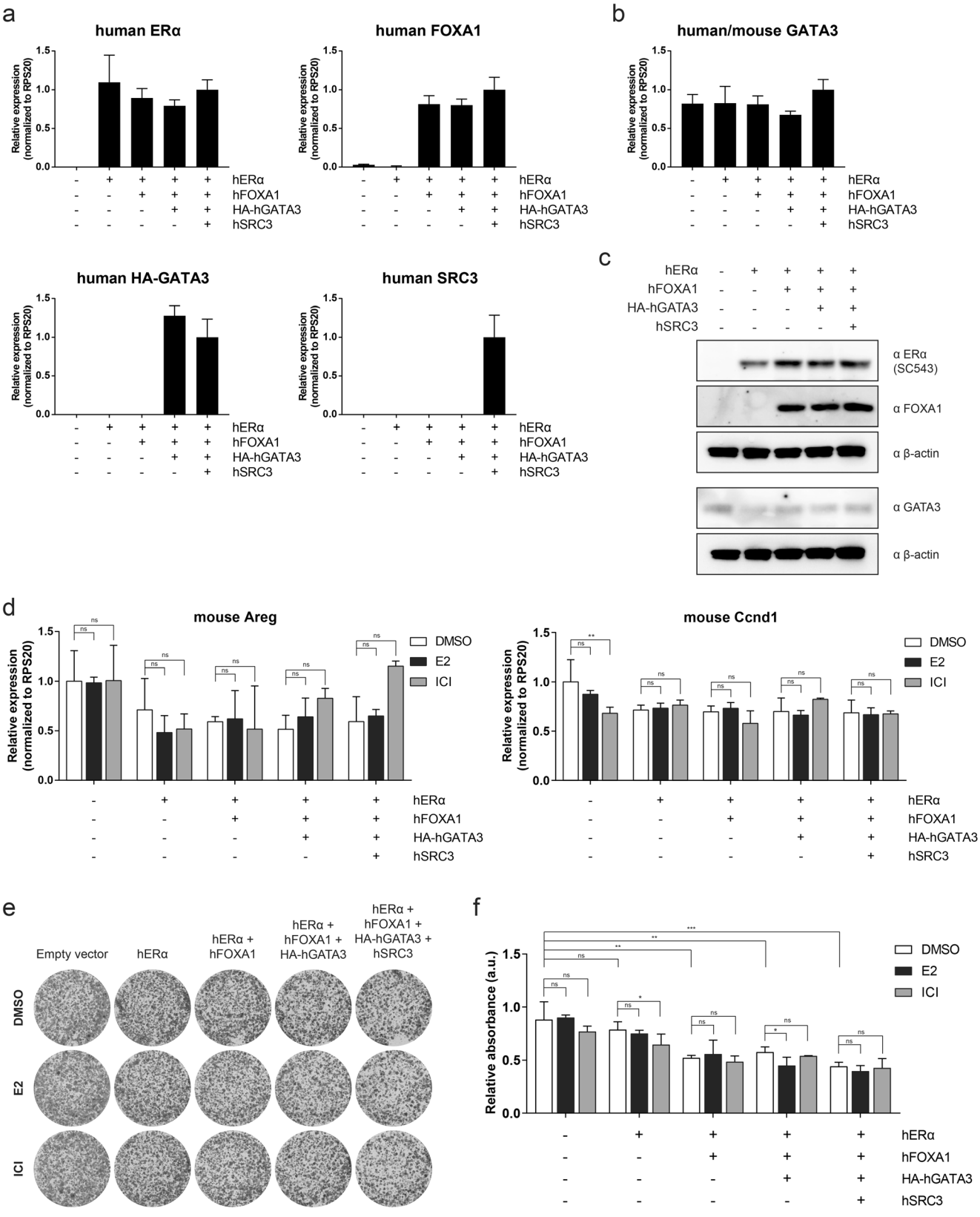

mice develop mammary tumors, of which the majority are ERα- and FOXA1-positive [66]. Transplantation of p53 null mammary epithelium results in tumor formation in about half of the recipient mice, which can be promoted by estradiol stimulation and inhibited by ovariectomy or tamoxifen treatment, but the majority of tumors that develop are ERα-negative [67–69].

◀ **Fig. 5** Expression of human ERα in combination with the transcription factors FOXA1, GATA3 and SRC3 does not sensitize mouse HC11 cells to ERα stimulation or inhibition. **a** RT-qPCR analysis using primers specific for human ERα, FOXA1, HA-tagged GATA3 and SRC3 in HC11 cells transduced with lentiviral constructs containing the indicated cDNAs. Data represent mean + SD, $n = 3$. **b** RT-qPCR analysis using primers recognizing both mouse and human GATA3 in HC11 cells transduced with lentiviral constructs containing the indicated cDNAs. Data represent mean + SD, $n = 3$. **c** Protein expression of human ERα and total FOXA1 and GATA3. β-actin was used as a loading control. **d** RT-qPCR analysis using primers specific for mouse *Areg* (*left*) and mouse *Ccnd1* (*right*) in HC11 cells transduced with lentiviral constructs containing the indicated cDNAs after stimulation with DMSO, E2 or ICI. Data represent mean + SD, $n = 2$. Two-way ANOVA: *Ccnd1*: Empty vector DMSO versus ICI, $p = 0.0070$. ** $p < 0.01$, ns $p > 0.05$. **e**,**f** Representative images (**e**) and quantification (**f**) of clonogenic assays of HC11 cells transduced with lentiviral constructs containing the indicated cDNAs and treated with DMSO, E2 or ICI. Data represent mean + SD, $n = 2$. Two-way ANOVA: hERα DMSO versus ICI, $p = 0.0270$; hERα/hFOXA1/HA-hGATA3 DMSO versus E2, $p = 0.0421$; Empty vector DMSO versus hERα/hFOXA1 DMSO, $p = 0.0021$; Empty vector DMSO versus hERα/hFOXA1/HA-hGATA3 DMSO, $p = 0.0071$; Empty vector DMSO versus hERα/hFOXA1/HA-hGATA3/hSRC3 DMSO, $p = 0.0004$. *** $p < 0.001$, ** $p < 0.01$, * $p < 0.05$, ns $p > 0.05$

Pregnancy-induced expression of $Kras^{G12V}$ in the mammary gland gives rise to luminal tumors that express ERα, where re-transplantation of a tumor derived cell line shows in vivo estrogen-dependency [70]. Even though these GEMMs with ERα-expressing mammary tumors are described, most of these models do not consistently give rise to ERα-positive mammary tumors and many are not shown to recapitulate ERα-dependency. In addition, not all genetic alterations that induce these ERα-expressing tumors are relevant for human luminal breast cancer. It remains therefore important to develop in vivo models of ERα-positive breast cancer that recapitulate their human counterparts more consistently.

Our data suggest that there are species-specific differences in ERα pioneer factor dependency that potentially hamper the development of ERα-positive mammary tumors in mice. We observed an absence of Forkhead motifs enriched at mouse ERα binding sites, but presence of Forkhead motifs at the human ERα binding sites, pointing towards species-specific differences that dictate the pioneer factor dependency of ERα. The underrepresentation of Forkhead motifs at ERα binding sites in murine cells cannot be explained by low expression levels of FOXA1, which has been shown to be expressed in the mouse mammary gland to a similar extent as ERα, and required for normal mammary gland development [71, 72]. The notion that species-specific differences between the mouse and human genome result in an altered ERα-cistrome is supported by the fact that transcription factors that are highly conserved in structure and function between mouse and human, show DNA binding patterns that appear to be largely species-specific [73]. Introduction of a human chromosome into the mouse genome results in a differential binding pattern of the same transcription factor on either the human or corresponding mouse gene locus, indicating that binding is directed by the DNA sequence rather than the transcription factor [74]. In addition, it has been shown that enhancers undergo rapid evolution, resulting in a relatively low conservation of enhancer regions between species [75]. It is therefore conceivable that differences between mouse and human genomes underlie species-specific differences in the transcriptional response to ERα-signaling, raising the question whether the mouse genome is primed for ERα-regulation in a similar fashion as the human genome.

Our study has certain limitations that are noteworthy. The first limitation is the use of a p53-deficient background to model ERα-positive breast cancer. Although *TP53* mutations occur in about 20–30% of ERα-positive luminal breast cancers, they are more common in ERα-negative basal cancers (80%) [22, 23]. Even though it was reported that a subset of mouse mammary tumors driven by mutation or loss of p53 express ERα [67, 68, 76, 77], our mouse model of p53-deficient breast cancer predominantly develops ERα-negative basal like mammary tumors [24], and expression of exogenous ERα in the mammary epithelium does not affect hormonal status of these tumors. In addition, while heterozygous loss of p53 together with ERα overexpression was reported to increase the risk of preneoplasia development in mice [78], we did not observe accelerated tumor formation in our p53-deficient breast cancer model upon exogenous ERα expression in the mammary epithelium. This suggests that whereas reduced p53 levels predispose for ERα-expression induced neoplastic growth, complete loss of p53 is a strong driver of tumor growth independent of ERα expression. In contrast to *TP53* mutations, *PIK3CA* mutations are more frequently observed in ERα-positive luminal breast cancers than in ERα-negative basal tumors [22, 23]. Recently it was shown that $Pik3ca^{H1047R}$-induced mammary tumors are ERα-positive, although it remains elusive whether these tumors are truly estrogen-dependent [79]. This suggests that mouse models of *Pik3ca*-mutated breast cancer might be a better starting point to develop models of ERα-driven breast cancer.

Another potential limitation is that transcription of ERα appeared to be silenced. However, in previous studies we successfully used this system to introduce expression of breast cancer drivers in the mouse mammary gland that resulted in efficient tumor formation [29, 80]. This suggests that silencing of the ERα knock-in alleles is promoted by negative selection pressure against ERα-expressing cells. A third limitation is the in vitro setting we used to test functionality of ERα, FOXA1 and GATA3 expression in mouse mammary epithelial cells, since there is no suitable ERα-expressing healthy breast cell model to compare our results to. Even though Kong et al. have shown that these human proteins stimulated ERα-dependent growth of human breast cancer cells [53], we were unable to induce ERα-dependent growth in primary mouse healthy mammary epithelial cells and the HC11 cell line using human ERα, FOXA1 and GATA3 protein expression. We cannot exclude that expression of mouse proteins will affect ERα-responsiveness more

efficiently in this system. In addition, expression of human ERα, FOXA1 and GATA3 might have a different outcome in healthy human breast cells than in human breast cancer cells. ERα-expressing cells and the proliferating cells are not the same population in healthy breast epithelium, in contrast to human breast cancer cells [81–83]. ERα is shown to induce expression of paracrine factors, such as *AREG*, that induce proliferation of adjacent mammary epithelial cells [84, 85]. Therefore, ERα expression in normal mammary epithelial cells does not necessarily induce proliferation, but might induce production of growth-stimulating paracrine factors. However, we also did not observe an increase in *Areg* production upon expression of human ERα, FOXA1 and GATA3. Even though expression of ERα, FOXA1 and GATA3 is not sufficient to induce ERα-dependency in mammary epithelial cells, all three factors are shown to be essential in development of mouse mammary gland [71, 86–88].

In conclusion, we have shown that expression of exogenous mouse or human ERα in mouse mammary epithelium is lost over time and does not accelerate the formation of p53-deficient mammary tumors. Pioneer factor dependency of ERα for DNA binding appears not to be conserved between the mouse and human genome and exogenously-introduced ERα, FOXA1 and GATA3 are not sufficient to induce ERα-dependency in MMECs, while this was reported to be the case in human triple-negative breast cancer cells [53]. Altogether, these results point towards species-specific differences between the mouse and human genome that result in an altered transcription factor dependency, which might hamper the utility of mouse models in ERα-positive breast cancer research. In contrast to mice, certain rat strains develop spontaneous and chemically-induced mammary tumors that recapitulate the ERα-positivity and estrogen-dependent growth of human luminal breast cancer [89–91]. These rat strains might therefore constitute more relevant in vivo models of ERα-positive breast cancer.

Acknowledgements We are grateful to Eline van der Burg, Ute Boon, Renske de Korte-Grimmerink, Micha Nethe and Yongsoo Kim for their technical support with the experiments. We thank the Netherlands Cancer Institute Genomics Core Facility, Mouse Clinic for Cancer and Aging, Animal Facility, and Animal Pathology Facility for their expert technical support.

GEO accession number: GSE127863.

Author Contributions LMC, LH, WZ and JJ designed research. LMC, LH, AD and ES performed research. LMC, LH, RB, SK, WZ and JJ analyzed data. LMC, WZ and JJ wrote the paper.

Funding Information This work was financially supported by the Oncode Institute; the Center for Translational Molecular Medicine (CTMM) Breast Care Project; the Netherlands Organization for Scientific Research (NWO: Cancer Genomics Netherlands (CGCNL), Cancer Systems Biology Center (CSBC), Zenith 93,512,009, Vici 91,814,643); the EU Seventh Framework Program (EurocanPlatform project 260,791); the European Research Council (ERC Synergy project CombatCancer); and a National Roadmap grant for Large-Scale Research facilities from NWO.

Compliance with Ethical Standards

Conflict of Interest The authors declare that there are no conflicts of interest.

References

1. Bray F, Ferlay J, Soerjomataram I, Siegel RL, Torre LA, Jemal A. Global cancer statistics 2018: GLOBOCAN estimates of incidence and mortality worldwide for 36 cancers in 185 countries. CA Cancer J Clin. 2018;68:394–424.
2. Perou CM, Sørlie T, Eisen MB, van de Rijn M, Jeffrey SS, Rees CA, et al. Molecular portraits of human breast tumours. Nature. 2000;406:747–52.
3. Sørlie T, Perou CM, Tibshirani R, Aas T, Geisler S, Johnsen H, et al. Gene expression patterns of breast carcinomas distinguish tumor subclasses with clinical implications. Proc Natl Acad Sci U S A. 2001;98:10869–74.
4. Brünner N, Bronzert D, Vindeløv LL, Rygaard K, Spang-Thomsen M, Lippman ME. Effect on growth and cell cycle kinetics of estradiol and tamoxifen on MCF-7 human breast cancer cells grown in vitro and in nude mice. Cancer Res. 1989;49:1515–20.
5. Arnal J-F, Lenfant F, Metivier R, Flouriot G, Henrion D, Adlanmerini M, et al. Membrane and nuclear estrogen receptor alpha actions: from tissue specificity to medical implications. Physiol Rev. 2017;97:1045–87.
6. Gruber CJ, Tschugguel W, Schneeberger C, Huber JC. Production and actions of estrogens. N Engl J Med. 2002;346:340–52.
7. Kumar R, Zakharov MN, Khan SH, Miki R, Jang H, Toraldo G, et al. The dynamic structure of the estrogen receptor. J Amino Acids. 2011;2011:812540.
8. Zaret KS, Carroll JS. Pioneer transcription factors: establishing competence for gene expression. Genes Dev. 2011;25:2227–41.
9. Hurtado A, Holmes KA, Ross-Innes CS, Schmidt D, Carroll JS. FOXA1 is a key determinant of estrogen receptor function and endocrine response. Nat Genet. 2011;43:27–33.
10. Theodorou V, Stark R, Menon S, Carroll JS. GATA3 acts upstream of FOXA1 in mediating ESR1 binding by shaping enhancer accessibility. Genome Res. 2013;23:12–22.
11. Kushner PJ, Agard DA, Greene GL, Scanlan TS, Shiau AK, Uht RM, et al. Estrogen receptor pathways to AP-1. J Steroid Biochem Mol Biol. 2000;74:311–7.
12. Safe S. Transcriptional activation of genes by 17 beta-estradiol through estrogen receptor-Sp1 interactions. Vitam Horm. 2001;62:231–52.
13. McKenna NJ, Lanz RB, O'Malley BW. Nuclear receptor coregulators: cellular and molecular biology. Endocr Rev. 1999;20:321–44.
14. Wärnmark A, Treuter E, Wright APH, Gustafsson J-Å. Activation functions 1 and 2 of nuclear receptors: molecular strategies for transcriptional activation. Mol Endocrinol. 2003;17:1901–9.
15. Yaşar P, Ayaz G, User SD, Güpür G, Muyan M. Molecular mechanism of estrogen–estrogen receptor signaling. Reprod Med Biol. 2017;16:4–20.
16. Xu J, Wu R-C, O'Malley BW. Normal and cancer-related functions of the p160 steroid receptor co-activator (SRC) family. Nat Rev Cancer. 2009;9:615–30.
17. Özdemir BC, Sflomos G, Brisken C. The challenges of modeling hormone receptor-positive breast cancer in mice. Endocr Relat Cancer. 2018;25:R319–30.
18. Osborne CK, Hobbs K, Clark GM. Effect of estrogens and antiestrogens on growth of human breast cancer cells in athymic nude mice. Cancer Res. 1985;45:584–90.

19. Wagner K-U. Models of breast cancer: quo vadis, animal modeling? Breast Cancer Res. 2004;6:31–8.
20. Vargo-Gogola T, Rosen JM. Modelling breast cancer: one size does not fit all. Nat Rev Cancer. 2007;7:659–72.
21. Dabydeen SA, Furth PA. Genetically engineered ERα-positive breast cancer mouse models. Endocr Relat Cancer. 2014;21: R195–208.
22. Cancer Genome Atlas Network. Comprehensive molecular portraits of human breast tumours. Nature. 2012;490:61–70.
23. Ciriello G, Gatza ML, Beck AH, Wilkerson MD, Rhie SK, Pastore A, et al. Comprehensive molecular portraits of invasive lobular breast cancer. Cell. 2015;163:506–19.
24. Derksen PWB, Braumuller TM, van der Burg E, Hornsveld M, Mesman E, Wesseling J, et al. Mammary-specific inactivation of E-cadherin and p53 impairs functional gland development and leads to pleomorphic invasive lobular carcinoma in mice. Dis Model Mech. 2011;4:347–58.
25. Jonkers J, Meuwissen R, van der Gulden H, Peterse H, van der Valk M, Berns A. Synergistic tumor suppressor activity of BRCA2 and p53 in a conditional mouse model for breast cancer. Nat Genet. 2001;29:418–25.
26. Huijbers IJ, Del Bravo J, Bin Ali R, Pritchard C, Braumuller TM, van Miltenburg MH, et al. Using the GEMM-ESC strategy to study gene function in mouse models. Nat Protoc. 2015;10:1755–85.
27. Henneman L, van Miltenburg MH, Michalak EM, Braumuller TM, Jaspers JE, Drenth AP, et al. Selective resistance to the PARP inhibitor olaparib in a mouse model for BRCA1-deficient metaplastic breast cancer. Proc Natl Acad Sci U S A. 2015;112:8409–14.
28. Boelens MC, Nethe M, Klarenbeek S, de Ruiter JR, Schut E, Bonzanni N, et al. PTEN loss in E-cadherin-deficient mouse mammary epithelial cells rescues apoptosis and results in development of classical invasive lobular carcinoma. Cell Rep. 2016;16:2087–101.
29. Kas SM, de Ruiter JR, Schipper K, Annunziato S, Schut E, Klarenbeek S, et al. Insertional mutagenesis identifies drivers of a novel oncogenic pathway in invasive lobular breast carcinoma. Nat Genet. 2017;49:1219–30.
30. Follenzi A, Ailles LE, Bakovic S, Geuna M, Naldini L. Gene transfer by lentiviral vectors is limited by nuclear translocation and rescued by HIV-1 *pol* sequences. Nat Genet. 2000;25:217–22.
31. Trapnell C, Pachter L, Salzberg SL. TopHat: discovering splice junctions with RNA-Seq. Bioinforma Oxf Engl. 2009;25:1105–11.
32. Langmead B, Trapnell C, Pop M, Salzberg SL. Ultrafast and memory-efficient alignment of short DNA sequences to the human genome. Genome Biol. 2009;10:R25.
33. Li H, Handsaker B, Wysoker A, Fennell T, Ruan J, Homer N, et al. The sequence alignment/map format and SAMtools. Bioinforma Oxf Engl. 2009;25:2078–9.
34. Anders S, Pyl PT, Huber W. HTSeq – a Python framework to work with high-throughput sequencing data. Bioinforma Oxf Engl. 2015;31:166–9.
35. Anders S, Huber W. Differential expression analysis for sequence count data. Genome Biol. 2010;11:R106.
36. Singh AA, Schuurman K, Nevedomskaya E, Stelloo S, Linder S, Droog M, et al. Optimized ChIP-seq method facilitates transcription factor profiling in human tumors. Life Sci Alliance. 2019;2: e201800115.
37. Zhang Y, Liu T, Meyer CA, Eeckhoute J, Johnson DS, Bernstein BE, et al. Model-based analysis of ChIP-Seq (MACS). Genome Biol. 2008;9:R137.
38. Kumar V, Muratani M, Rayan NA, Kraus P, Lufkin T, Ng HH, et al. Uniform, optimal signal processing of mapped deep-sequencing data. Nat Biotechnol. 2013;31:615–22.
39. Ye T, Krebs AR, Choukrallah M-A, Keime C, Plewniak F, Davidson I, et al. seqMINER: an integrated ChIP-seq data interpretation platform. Nucleic Acids Res. 2011;39:e35.
40. Ji X, Li W, Song J, Wei L, Liu XS. CEAS: cis -regulatory element annotation system. Nucleic Acids Res. 2006;34:W551–4.
41. Liu T, Ortiz JA, Taing L, Meyer CA, Lee B, Zhang Y, et al. Cistrome: an integrative platform for transcriptional regulation studies. Genome Biol. 2011;12:R83.
42. Battersby S, Robertson B, Anderson T, King R, McPherson K. Influence of menstrual cycle, parity and oral contraceptive use on steroid hormone receptors in normal breast. Br J Cancer. 1992;65: 601–7.
43. Goyal R, Gupta T, Gupta R, Aggarwal A, Sahni D, Singh G. Histological and immunohistochemical study of estrogen and progesterone receptors in normal human breast tissue in adult age groups vulnerable to malignancy: histological and IHC study of ER and PR in normal breast tissue. Clin Anat. 2016;29:729–37.
44. Nilsson ME, Vandenput L, Tivesten Å, Norlén A-K, Lagerquist MK, Windahl SH, et al. Measurement of a comprehensive sex steroid profile in rodent serum by high-sensitive gas chromatography-tandem mass spectrometry. Endocrinology. 2015;156:2492–502.
45. van de Ven M, Liu X, van der Burg E, Klarenbeek S, Alexi X, Zwart W, et al. BRCA1-associated mammary tumorigenesis is dependent on estrogen rather than progesterone signaling. J Pathol. 2018;246:41–53.
46. Zwart W, Theodorou V, Kok M, Canisius S, Linn S, Carroll JS. Oestrogen receptor–co-factor–chromatin specificity in the transcriptional regulation of breast cancer. EMBO J. 2011;30:4764–76.
47. Usary J, Llaca V, Karaca G, Presswala S, Karaca M, He X, et al. Mutation of GATA3 in human breast tumors. Oncogene. 2004;23: 7669–78.
48. Jansen MPHM, Knijnenburg T, Reijm EA, Simon I, Kerkhoven R, Droog M, et al. Hallmarks of aromatase inhibitor drug resistance revealed by epigenetic profiling in breast cancer. Cancer Res. 2013;73:6632–41.
49. Droog M, Nevedomskaya E, Dackus GM, Fles R, Kim Y, Hollema H, et al. Estrogen receptor α wields treatment-specific enhancers between morphologically similar endometrial tumors. Proc Natl Acad Sci U S A. 2017;114:E1316–25.
50. Chi D, Singhal H, Li L, Xiao T, Liu W, Pun M, et al. Estrogen receptor signaling is reprogrammed during breast tumorigenesis. Proc Natl Acad Sci U S A. 2019;116:11437–43.
51. Nautiyal J, Steel JH, Mane MR, Oduwole O, Poliandri A, Alexi X, et al. The transcriptional co-factor RIP140 regulates mammary gland development by promoting the generation of key mitogenic signals. Development. 2013;140:1079–89.
52. Hewitt SC, Li L, Grimm SA, Chen Y, Liu L, Li Y, et al. Research resource: whole-genome estrogen receptor α binding in mouse uterine tissue revealed by ChIP-seq. Mol Endocrinol Baltim Md. 2012;26:887–98.
53. Kong SL, Li G, Loh SL, Sung W-K, Liu ET. Cellular reprogramming by the conjoint action of ERα, FOXA1, and GATA3 to a ligand-inducible growth state. Mol Syst Biol. 2011;7:526.
54. Nilsson S, Mäkelä S, Treuter E, Tujague M, Thomsen J, Andersson G, et al. Mechanisms of estrogen action. Physiol Rev. 2001;81: 1535–65.
55. Chou J, Lin JH, Brenot A, Kim J, Provot S, Werb Z. GATA3 suppresses metastasis and modulates the tumour microenvironment by regulating microRNA-29b expression. Nat Cell Biol. 2013;15: 201–13.
56. Yan W, Cao QJ, Arenas RB, Bentley B, Shao R. GATA3 inhibits breast cancer metastasis through the reversal of epithelial-mesenchymal transition. J Biol Chem. 2010;285:14042–51.
57. Peterson EA, Jenkins EC, Lofgren KA, Chandiramani N, Liu H, Aranda E, et al. Amphiregulin is a critical downstream effector of estrogen signaling in ERα-positive breast cancer. Cancer Res. 2015;75:4830–8.

58. Altucci L, Addeo R, Cicatiello L, Dauvois S, Parker MG, Truss M, et al. 17beta-estradiol induces cyclin D1 gene transcription, p36D1-p34cdk4 complex activation and p105Rb phosphorylation during mitogenic stimulation of G(1)-arrested human breast cancer cells. Oncogene. 1996;12:2315–24.
59. Howell A, Osborne CK, Morris C, Wakeling AE. ICI 182,780 (Faslodex™). Cancer. 2000;89:817–25.
60. Tilli MT, Frech MS, Steed ME, Hruska KS, Johnson MD, Flaws JA, et al. Introduction of estrogen receptor-α into the tTA/TAg conditional mouse model precipitates the development of estrogen-responsive mammary adenocarcinoma. Am J Pathol. 2003;163:1713–9.
61. Torres-Arzayus MI, de Mora JF, Yuan J, Vazquez F, Bronson R, Rue M, et al. High tumor incidence and activation of the PI3K/AKT pathway in transgenic mice define AIB1 as an oncogene. Cancer Cell. 2004;6:263–74.
62. Torres-Arzayus MI, Zhao J, Bronson R, Brown M. Estrogen-dependent and independent-mechanisms contribute to AIB1-mediated tumor formation. Cancer Res. 2010;70:4102–11.
63. Chan SR, Vermi W, Luo J, Lucini L, Rickert C, Fowler AM, et al. STAT1-deficient mice spontaneously develop estrogen receptor α-positive luminal mammary carcinomas. Breast Cancer Res. 2012;14:R16.
64. Rose-Hellekant TA, Arendt LM, Schroeder MD, Gilchrist K, Sandgren EP, Schuler LA. Prolactin induces ERα-positive and ERα-negative mammary cancer in transgenic mice. Oncogene. 2003;22:4664–74.
65. Arendt LM, Rugowski DE, Grafwallner-Huseth TA, Garcia-Barchino MJ, Rui H, Schuler LA. Prolactin-induced mouse mammary carcinomas model estrogen resistant luminal breast cancer. Breast Cancer Res. 2011;13:R11.
66. Chen F, Li A, Gao S, Hollern D, Williams M, Liu F, et al. Tip30 controls differentiation of murine mammary luminal progenitor to estrogen receptor-positive luminal cell through regulating FoxA1 expression. Cell Death Dis. 2014;5:e1242.
67. Medina D, Kittrell FS, Shepard A, Stephens LC, Jiang C, Lu J, et al. Biological and genetic properties of the p53 null preneoplastic mammary epithelium. FASEB J. 2002;16:881–3.
68. Medina D, Kittrell FS, Hill J, Shepard A, Thordarson G, Brown P. Tamoxifen inhibition of estrogen receptor-α–negative mouse mammary tumorigenesis. Cancer Res. 2005;65:3493–6.
69. Mazumdar A, Medina D, Kittrell FS, Zhang Y, Hill JL, Edwards DE, et al. The combination of tamoxifen and the rexinoid LG100268 prevents ER-positive and ER-negative mammary tumors in p53-null mammary gland mice. Cancer Prev Res (Phila Pa). 2012;5:1195–202.
70. Andò S, Malivindi R, Catalano S, Rizza P, Barone I, Panza S, et al. Conditional expression of Ki-RasG12V in the mammary epithelium of transgenic mice induces estrogen receptor alpha (ERα)-positive adenocarcinoma. Oncogene. 2017;36:6420–31.
71. Bernardo GM, Lozada KL, Miedler JD, Harburg G, Hewitt SC, Mosley JD, et al. FOXA1 is an essential determinant of ERα expression and mammary ductal morphogenesis. Development. 2010;137:2045–54.
72. Besnard V, Wert SE, Hull WM, Whitsett JA. Immunohistochemical localization of Foxa1 and Foxa2 in mouse embryos and adult tissues. Gene Expr Patterns GEP. 2004;5:193–208.
73. Odom DT, Dowell RD, Jacobsen ES, Gordon W, Danford TW, MacIsaac KD, et al. Tissue-specific transcriptional regulation has diverged significantly between human and mouse. Nat Genet. 2007;39:730–2.
74. Wilson MD, Barbosa-Morais NL, Schmidt D, Conboy CM, Vanes L, Tybulewicz VLJ, et al. Species-specific transcription in mice carrying human chromosome 21. Science. 2008;322:434–8.
75. Villar D, Berthelot C, Aldridge S, Rayner TF, Lukk M, Pignatelli M, et al. Enhancer evolution across 20 mammalian species. Cell. 2015;160:554–66.
76. Lin S-CJ, Lee K-F, Nikitin AY, Hilsenbeck SG, Cardiff RD, Li A, et al. Somatic mutation of p53 leads to estrogen receptor α-positive and -negative mouse mammary tumors with high frequency of metastasis. Cancer Res. 2004;64:3525–32.
77. Wijnhoven SWP, Zwart E, Speksnijder EN, Beems RB, Olive KP, Tuveson DA, et al. Mice expressing a mammary gland–specific R270H mutation in the p53 tumor suppressor gene mimic human breast cancer development. Cancer Res. 2005;65:8166–73.
78. Díaz-Cruz ES, Furth PA. Deregulated estrogen receptor α and p53 heterozygosity collaborate in the development of mammary hyperplasia. Cancer Res. 2010;70:3965–74.
79. Stratikopoulos EE, Kiess N, Szabolcs M, Pegno S, Kakit C, Wu X, et al. Mouse ER+/PIK3CA H1047R breast cancers caused by exogenous estrogen are heterogeneously dependent on estrogen and undergo BIM-dependent apoptosis with BH3 and PI3K agents. Oncogene. 2019;38:47–59.
80. Annunziato S, Kas SM, Nethe M, Yücel H, Bravo JD, Pritchard C, et al. Modeling invasive lobular breast carcinoma by CRISPR/Cas9-mediated somatic genome editing of the mammary gland. Genes Dev. 2016;30:1470–80.
81. Clarke RB, Howell A, Potten CS, Anderson E. Dissociation between steroid receptor expression and cell proliferation in the human breast. Cancer Res. 1997;57:4987–91.
82. Clarke RB. Complementary yet distinct roles for oestrogen receptor-α and oestrogen receptor-β in mouse mammary epithelial proliferation. Breast Cancer Res. 2004;6:135–6.
83. Russo J, Ao X, Grill C, Russo IH. Pattern of distribution of cells positive for estrogen receptor a and progesterone receptor in relation to proliferating cells in the mammary gland. Breast Cancer Res Treat. 1999;53:217–27.
84. Mallepell S, Krust A, Chambon P, Brisken C. Paracrine signaling through the epithelial estrogen receptor a is required for proliferation and morphogenesis in the mammary gland. Proc Natl Acad Sci U S A. 2006;103:2196–201.
85. Ciarloni L, Mallepell S, Brisken C. Amphiregulin is an essential mediator of estrogen receptor α function in mammary gland development. Proc Natl Acad Sci U S A. 2007;104:5455–60.
86. Bocchinfuso WP, Korach KS. Mammary gland development and tumorigenesis in estrogen receptor knockout mice. J Mammary Gland Biol Neoplasia. 1997;2:323–34.
87. Kouros-Mehr H, Slorach EM, Sternlicht MD, Werb Z. GATA-3 maintains the differentiation of the luminal cell fate in the mammary gland. Cell. 2006;127:1041–55.
88. Asselin-Labat M-L, Sutherland KD, Barker H, Thomas R, Shackleton M, Forrest NC, et al. Gata-3 is an essential regulator of mammary-gland morphogenesis and luminal-cell differentiation. Nat Cell Biol. 2007;9:201–9.
89. Russo J, Gusterson BA, Rogers AE, Russo IH, Wellings SR, van Zwieten MJ. Comparative study of human and rat mammary tumorigenesis. Lab Investig J Tech Methods Pathol. 1990;62:244–78.
90. Nandi S, Guzman RC, Yang J. Hormones and mammary carcinogenesis in mice, rats, and humans: a unifying hypothesis. Proc Natl Acad Sci U S A. 1995;92:3650–7.
91. Shull JD, Dennison KL, Chack AC, Trentham-Dietz A. Rat models of 17β-estradiol-induced mammary cancer reveal novel insights into breast cancer etiology and prevention. Physiol Genomics. 2018;50:215–34.

Affiliations

Lisette M. Cornelissen[1] · Linda Henneman[1,2] · Anne Paulien Drenth[1] · Eva Schut[1] · Roebi de Bruijn[1,3] · Sjoerd Klarenbeek[4] · Wilbert Zwart[5,6] · Jos Jonkers[1]

[1] Division of Molecular Pathology, The Netherlands Cancer Institute, Plesmanlaan 121, 1066CX Amsterdam, The Netherlands

[2] Mouse Clinic for Cancer and Aging – Transgenic facility, The Netherlands Cancer Institute, Plesmanlaan 121, Amsterdam 1066CX, The Netherlands

[3] Division of Molecular Carcinogenisis, Oncode Institute, The Netherlands Cancer Institute, Plesmanlaan 121, Amsterdam 1066CX, The Netherlands

[4] Experimental Animal Pathology, The Netherlands Cancer Institute, Plesmanlaan 121, Amsterdam 1066CX, The Netherlands

[5] Division of Oncogenomics, Oncode Institute, The Netherlands Cancer Institute, Plesmanlaan 121, 1066CX Amsterdam, The Netherlands

[6] Laboratory of Chemical Biology and Institute for Complex Molecular Systems, Department of Biomedical Engineering, Eindhoven University of Technology, PO Box 513, Eindhoven, The Netherlands